Seasonal controls on the exchange of carbon and water in an Amazonian rain forest

Lucy R. Hutyra,[1,2] J. William Munger,[1,3] Scott R. Saleska,[4] Elaine Gottlieb,[1,3] Bruce C. Daube,[1,3] Allison L. Dunn,[1,5,6] Daniel F. Amaral,[7] Plinio B. de Camargo,[8] and Steven C. Wofsy[1,3]

Received 7 November 2006; revised 1 April 2007; accepted 15 May 2007; published 1 August 2007.

[1] The long-term resilience of Amazonian forests to climate changes and the fate of their large stores of organic carbon depend on the ecosystem response to climate and weather. This study presents 4 years of eddy covariance data for CO_2 and water fluxes in an evergreen, old-growth tropical rain forest examining the forest's response to seasonal variations and to short-term weather anomalies. Photosynthetic efficiency declined late in the wet season, before appreciable leaf litter fall, and increased after new leaf production midway through the dry season. Rates of evapotranspiration were inelastic and did not depend on dry season precipitation. However, ecosystem respiration was inhibited by moisture limitations on heterotrophic respiration during the dry season. The annual carbon balance for this ecosystem was very close to neutral, with mean net loss of 890 ± 220 kg C ha^{-1} yr^{-1}, and a range of −221 ± 453 (C uptake) to +2677 ± 488 (C loss) kg C ha^{-1} yr^{-1} over 4 years. The trend from large net carbon release in 2002 towards net carbon uptake in 2005 implies recovery from prior disturbance. The annual carbon balance was sensitive to weather anomalies, particularly the timing of the dry-to-wet season transition, reflecting modulation of light inputs and respiration processes. Canopy carbon uptake rates were largely controlled by phenology and light with virtually no indication of seasonal water limitation during the 5-month dry season, indicating ample supplies of plant-available-water and ecosystem adaptation for maximum light utilization.

Citation: Hutyra, L. R., J. W. Munger, S. R. Saleska, E. Gottlieb, B. C. Daube, A. L. Dunn, D. F. Amaral, P. B. de Camargo, and S. C. Wofsy (2007), Seasonal controls on the exchange of carbon and water in an Amazonian rain forest, *J. Geophys. Res.*, *112*, G03008, doi:10.1029/2006JG000365.

1. Introduction

[2] Tropical forests are closely coupled to climate, exerting a strong influence on temperature and precipitation patterns whilst these same weather and climate patterns dictate where particular forest types can establish and persist [*Holdridge*, 1947]. The interactions between regional and global climate and the Amazonian rain forest are uncertain. Both model results and field studies show wide variability in the spatial patterns and seasonality of forest growth, respiration, and water exchange [e.g., *Saleska et al.*, 2003; *Schaphoff et al.*, 2006]. Mechanistic understanding of the forest responses to climatic factors (particularly temperature, light, and moisture) is required to improve ecosystem process models for tropical forests and to enable more accurate projections of possible responses to changes in climate.

[3] The Amazon Basin accounts for 50% of the world's undisturbed tropical rain forest [*FAO*, 1992], 10% of global terrestrial net primary productivity [*Melillo et al.*, 1993], and a major portion of the global surface evaporation [*Choudhury and DiGirolamo*, 1998]. Much of the Amazon maintains a green canopy throughout the dry season by acquiring water through deep roots [*Nepstad et al.*, 1994] and possibly by hydraulic redistribution of water by plants [*Oliveira et al.*, 2005]. *Huete et al.* [2006] found widescale 'green-up' of Amazonian rain forest during the dry season, with new leaf production during the period of maximum temperature, the most sunlight, and minimum precipitation.

[4] Previous Amazonian studies have reported diverse seasonal patterns in the net ecosystem exchange of CO_2 from forests. Some sites found enhanced uptake of CO_2 during the dry season [*Saleska et al.*, 2003; *Goulden et al.*, 2004], others reported decreased uptake during the dry season [*Malhi et al.*,

[1]Department of Earth and Planetary Sciences, Harvard University, Cambridge, Massachusetts, USA.
[2]Now at Department of Urban Design and Planning, University of Washington, Seattle, Washington, USA.
[3]School of Engineering and Applied Sciences, Harvard University, Cambridge, Massachusetts, USA.
[4]Department of Ecology and Evolutionary Biology, University of Arizona, Tucson, Arizona, USA.
[5]Department of Soil Sciences, University of Manitoba, Winnipeg, Manitoba, Canada.
[6]Department of Physical and Earth Sciences, Worcester State College, Worcester, Massachusetts, USA.
[7]LBA-ECO, Santarém, Pará, Brazil.
[8]Laboratório de Ecologia Isotópica, CENA/USP, Piracicaba, Sao Paulo, Brazil.

0148-0227/07/2006JG000365

1998; *Araújo et al.*, 2002; *von Randow et al.*, 2004], and others showed no seasonality in the exchange patterns [*Carswell et al.*, 2002]. A data-model comparison for the Tapajós National Forest found that the Terrestrial Ecosystem Model (TEM) [*Tian et al.*, 1998] and Integrated Biosphere Simulator (IBIS) [*Botta et al.*, 2002] model predicted seasonality opposite to observed patterns [*Saleska et al.*, 2003]. Net carbon uptake was observed in the dry season due to lower seasonal respiration rates [*Saleska et al.*, 2003], whereas models predicted carbon release in the dry season due to water limitations on photosynthetic uptake of CO_2.

[5] Similarly, evapotranspiration (ET), the combination of surface evaporation and plant transpiration, has been found to peak at some forest sites during the dry season when radiation inputs were highest [*Hutyra et al.*, 2005; *da Rocha et al.*, 2004; *Carswell et al.*, 2002; *von Randow et al.*, 2004; *Shuttleworth*, 1988], but at other sites maximum ET occurred during the wet season when water availability was highest [*Malhi et al.*, 2002; *Vourlitis et al.*, 2002]. The observed divergence between sites is likely due to differences in the actual water available to the vegetation, plus differences in phenology and radiative drivers. The amount of moisture available to a forest affects the forest's physical structure, ecophysiology, and flammability. Moisture availability is a function of not only incoming precipitation, but also the depth and texture of the soil, the depth of the water table, transpiration demands of the forest, soil capillarity, site hydrology, and the vertical distribution of roots. Drier forests can behave like moister forests if deep roots and/or favorable soils provide access to water throughout the dry season months.

[6] Global Climate Models (GCM) generally predict decreases in Amazonian ET during the dry season, in phase with precipitation [*Dickinson and Henderson-Sellers*, 1988; *Werth and Avissar*, 2004]. *Lee et al.* [2005] updated the National Center for Atmospheric Research Community Atmospheric Model to include both hydraulic redistribution and deep roots in the Amazon. This model produced higher dry season ET relative to control runs, but ET still maximized during the wet season. Evidently we need better understanding of the controls on H_2O exchange in order to improve models to predict forest flammability and to forecast the effects of drought on forest species abundances, biomass distributions, and rates of photosynthesis and ecosystem respiration.

[7] To gain insight into the mechanisms controlling the exchange of carbon and water at the Tapajós old-growth forest, we first summarize observed local meteorology and energy exchange, and then present detailed methods, data processing techniques and validation strategies necessary for making accurate, unbiased eddy covariance measurements in a remote rain forest. We address two major scientific questions: (1) What are the controls on seasonal and inter-annual variations of net ecosystem exchange of CO_2, respiration, and photosynthesis, and water exchange? (2) Is forest growth water-limited during the dry season, or on an annual basis?

2. Methods

2.1. Site Description

[8] Our study was part of the Brazilian-led Large-Scale Biosphere-Atmosphere Experiment in Amazonia (LBA-ECO). The site is located in the Tapajós National Forest (TNF; 54°58′W, 2°51′S, Pará, Brazil) near Km 67 of the Santarém-Cuiabá highway (BR-163). The TNF is bounded by the Tapajós River to the west and the BR-163 highway on the east, extending from 50 km to 150 km south of the city of Santarém, Pará, Brazil. East of BR-163 the landscape is extensively developed for agriculture. The tower was located ~6 km west of the BR-163 highway and ~6 km east of the Tapajós River, in an area of largely contiguous forest extending for tens of kilometers to the north and south.

[9] The soils at this site are predominately nutrient-poor oxisols with pockets of sandy ultisols, both having low organic content and cation exchange capacity [*Silver et al.*, 2000]. During well drilling at a nearby site with similar soils, the water table was found to be at ~100 m depth [*Nepstad et al.*, 2002]. The forest is on flat terrain and has a closed canopy with a mean height of approximately 40–45 m and emergent trees reaching up to 55 m. There are few indications of recent anthropogenic disturbance other than small hunting trails. This forest can be classified as 'primary' with abundant large logs, numerous epiphytes, an uneven age distribution, and emergent trees [*Clark*, 1996]. Ground-based biometric plots were established at this site in July, 1999. See *Rice et al.* [2004] and *Vieira et al.* [2004] for more complete descriptions of the forest structure and growth dynamics.

2.2. Instrumentation

[10] A 64 m tower (Rohn 55G, Peoria, IL) was instrumented for eddy covariance measurements which commenced in April, 2001 and continued until the tower was destroyed when a falling tree hit the guy wires in January 2006. Three modular enclosures (approximately 1 m × 0.6 m × 0.2 m) containing all the key instruments and data loggers were mounted on the tower to keep inlet tubes short (~2 m) (Figure 1). Eddy-flux measurements were made at a height of 57.8 m with a sample rate of 8 Hz. A 3-axis sonic anemometer (CSAT-3, Campbell Scientific, Logan, UT) was mounted with the air sample inlet located 20 cm from the anemometer. The flux system drew sample air from the inlet through a 50 mm diameter Teflon filter and 9.5 mm (inner diameter) Teflon PFA tubing to a closed-path infrared gas analyzer (IRGA, LI-6262, Licor, Lincoln, NE). The eddy system sample cell (11.9 cm^3) was pressure-controlled at 66.6 kPa with a mass flow rate of 6000 sccm, providing a cell-flushing time of 0.078 s. This system design maintains the advantages of the closed-path sensor (e.g., precise instrument calibration, constant pressure and temperature), while also adding some of the advantages (e.g., minimal attenuation of high-frequency fluctuations) attributed to open-path designs. This system is particularly suitable for deployment with very tall vegetation where problems accrue due to long sample-tubes from the top of the tower.

[11] Calibrations of the eddy system for CO_2 were made every 6 hours (April 2001–November 11, 2002 and March 29, 2003–November 15, 2003) or 12 hours (November 12, 2002–March 29, 2003 and November 15, 2003–January 24, 2006) using 325, 400, and 475 ppm CO_2 standard gases traceable to world standards. The instrument was zeroed every 2 hours using a zero air generator (Parker Balston 74–5041, Haverhill, MA). The long-term accuracy of the instruments was ensured by measuring a surveillance standard (traceable to NOAA/CMDL standards at 380.45 ppm) once per week, this tank lasted through the duration of the

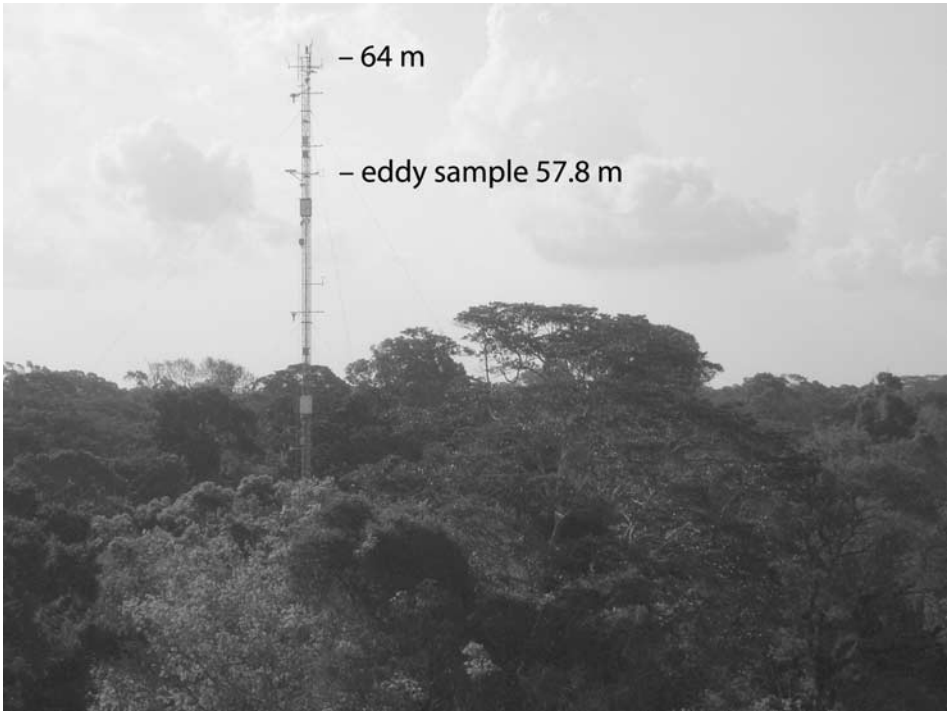

Figure 1. Eddy flux tower and forest canopy in the TNF.

measurements. Calibrations for water vapor were made using the daily fluctuations of $T_v - T_k$, where T_v is the sonic temperature (derived from the speed of sound provided by the sonic anemometer, closely approximating the virtual temperature) and T_k is the ambient temperature. This approach was necessary due to failures in the chilled mirror hygrometers originally installed for this purpose (see the auxiliary material for additional details about calibration methods).[1]

[12] Vertical profiles of CO_2 and H_2O concentrations were measured at 8 levels on the tower (62.2, 50, 39.4, 28.7, 19.6, 10.4, and 0.91 m). Sample air was drawn at 1000 sccm through the 8 profile inlets in sequence (2 minutes at each level). The profile concentration data were used to estimate the change in vertical average concentration between the ground and flux measurement height in order to calculate the column average storage of CO_2. The profile IRGA was zeroed between each profile sequence and an absolute calibration at 325, 400, and 475 ppm was made every 6 or 12 hours, as it was for the eddy CO_2 measurements.

[13] A suite of environmental measurements was also made on the tower (Table 1). Data loggers (CR-10X, Campbell Scientific, Logan, UT), controlled the overall operation of the system. The data were downloaded via coaxial cable to a computer, housed in a climate controlled hut near the tower.

2.3. Data Processing and Analysis

[14] The net ecosystem exchange (NEE) of CO_2 between the forest and the atmosphere was computed as

$$NEE = \overline{w'c'} + \frac{\partial}{\partial t}\int_0^h \overline{c(z)}dz \qquad (1)$$

where the first term on the right hand side is the covariance between vertical wind velocity fluctuations (w') and fluctuations in the concentration of the scalar (c', CO_2). The second term is the rate of change in the canopy storage, where z is the height above the ground surface, h is the flux measurement height, t is time, and the overbar denotes a time average [*Baldocchi et al.*, 1988]. The vertical coordinate for wind velocities is positive upward, thus positive values for fluxes denote emission and negative values denote uptake. Concentrations of CO_2 and H_2O were calculated using output from the IRGA's raw signal using a third order polynomial fit to the calibration data. CO_2 concentrations were corrected for water vapor. The temperature and pressure inside the sample cell were constant and thus no density fluctuation corrections were required (the data were represented as mole fraction in dry air [see *Webb et al.*, 1980]).

[15] Cospectral analyses of CO_2, H_2O, and heat flux measurements were done to assess the reliability of the flux data and to verify if appropriate averaging intervals have been used to capture all of the flux-carrying eddies [*Kaimal et al.*, 1972]. An ogive analysis [*Lee et al.*, 2004] provided an independent check on the adequacy of sampling intervals by looking for an asymptotic plateau in the cumulative sums of the cospectra (between 1 Hz and 34.2 minutes). The daytime ogives for CO_2, H_2O, and heat fluxes (Figure S1.) indicate that for this site a 30 minute averaging period was appropriate. We did not examine averaging intervals beyond 34.2 minutes due to the instrument calibration schedule, but the ogives indicate that the low frequency fluxes were adequately captured. There was some attenuation of high frequency (above 0.1 Hz) components of the water vapor flux due to adsorption and desorption along the sample tube walls and inlet filters, but attenuation losses were low (<2%) because of the short sample tube lengths. We corrected for

[1] Auxiliary materials are available in the HTML. doi:10.1029/2006JG000365.

Table 1. List of Environmental Measurements, Instruments, and Measurement Heights on the Tower

Measurement	Instrument	Height on Tower
Net radiation	Rebs Q7.1 with RV2 ventilation	64.1 m
Photosynthetically active radiation (PAR)	Licor 190-SA	63.6 m and 15.1 m
Aspirated air temperature	Met One 076B-4 aspirations with YSI 44032 thermistors	61.9, 49.8, 39.1, 28.4, 18.3, 10.1, 2.8, and 0.6 m
Atmospheric pressure	MKS 627A Baratron pressure transducer	Ground-level
Dew point hygrometers	EdgeTech 200M	57.9 m
Wind speed	Spinning cup anemometer, Met One 010C	64.1, 52, 38.2, and 30.7 m
Wind direction	Met One 020C	64.1 m
Precipitation	Texas Electronics 076B-4	42.6 m

attenuation as described by *Goulden et al.* [1996]. There may also be a small loss of water flux (<5%) at frequencies longer than 30 minutes, but we do not have a reliable method to account for that portion of the cospectrum.

[16] Eddy fluxes (CO_2, H_2O, momentum, and sensible heat) were calculated as 30-minute block averages, after rotating the wind field to a plane of zero mean vertical wind for each 30-minute period [*McMillen*, 1988], then averaged to hourly means. Time lags, due to sample travel time and adsorption in the sample line, were determined by maximizing the correlation between w' and c' and were found to be approximately 1 s and 2 s for CO_2 and H_2O, respectively. See the auxiliary material for more details about energy flux calculations and calibration methods.

[17] Rainy periods were not explicitly excluded in the processing. However, half-hourly data were filtered to exclude high rates of error in the sonic and IRGA error flags, typically attributable to heavy rainfall and extreme temperatures. We required a minimum of 70% and 20% IRGA and sonic data coverage, respectively, for each half-hour period to be included in the time series. This filtering had the effect of excluding periods of heavy rainfall. The sonic transducers were coated with hydrophobic grease and wicking material to minimize the down time after rain ended.

[18] ET and latent heat flux (LE) are both based on measurements of water vapor flux (F_{H2O}) and represent the sum of surface evaporation, condensation, and plant transpiration. LE is computed as the product of the latent heat of vaporization and the measured F_{H2O}, reported in energy units (W m^{-2}). ET is the sum of half-hourly net water vapor fluxes (F_{H2O}) reported in mm day^{-1} for analyses of water budget. Negative ET and LE fluxes denote condensation and positive ET and LE fluxes indicate evaporation plus transpiration.

[19] Measurements of NEE were separated into the component fluxes of ecosystem respiration (R) and gross primary production (GPP) in order to examine the mechanisms controlling the observed patterns of exchange. R was estimated using nighttime NEE measurements during well-mixed periods where the friction velocity,

$$u^* = \sqrt{-1^*\overline{w'u'}}, \tag{2}$$

was greater than or equal to 0.22 m s^{-1} (see section 3.5 for additional information on constraining R estimates). Figure S2 shows the relationship between nighttime NEE and u*. We have critically assessed potential errors and biases associated with lost nocturnal flux and missing canopy storage measurements at this site (L. R. Hutyra et al., Resolving systematic errors in estimates of net ecosystem exchange of CO_2 and ecosystem respiration in a tall-stature forest: Application to a tropical forest biome, submitted to *Agricultural and Forest Meteorology*, 2007, hereinafter referred to as Hutyra et al., submitted manuscript, 2007). This analysis strongly supports the appropriateness of the u* filter and the threshold value, using a suite of independent validation methods for both the NEE and R.

[20] Filling of data gaps was required to obtain a continuous time series for R. Filling for this data set was based on the mean nocturnal NEE within short, sub-seasonal intervals. The 4-year data set was divided into sample bins each containing 50 hours of well-mixed nighttime observations with a median sample bin size of 12 days. Values of R during the daytime and calm nighttime hours were estimated based on the mean of the valid nighttime observations within a given sample bin. We did not find a statistically significant correlation between R and nighttime temperature at this site within the gap-filling timescales (see section 4.3 for discussion about the temperature relationships). Therefore, the gap filling was based on mean nighttime NEE values, capturing seasonal patterns but not imposing any diel patterns on the R flux estimates.

[21] GPP refers to canopy carbon uptake such that

$$\mathrm{NEE} = \mathrm{R} - \mathrm{GPP}. \tag{3}$$

Since we use only nighttime observations to estimate R, the magnitude of daytime R should be considered a first order estimate. To obtain a continuous time series of GPP, the data set was divided into sample bins each containing 75 good hours of observations (well-mixed, daytime hours) and missing GPP values were replaced using a fit between GPP and photosynthetically active radiation (PAR). If the curvature in the relationship between GPP and PAR was significant (p-value $\leq$ 0.05), a hyperbolic fit was used, otherwise a linear fit was utilized. The hyperbolic fit was employed in 95% of the periods, with a linear fit being used when there was insufficient low light data to accurately capture the curvature in the GPP-light relationship. The median sample bin size was 8 days.

[22] From January 2002 to January 2006 CO_2 flux data were recorded for 81.2% of possible hours. After accounting for both weak atmospheric turbulence and instrument failures, 48.3% of all possible hours were utilized in this analysis. Missing NEE values were filled using the derived R and GPP estimates. The mean difference between the measured and derived NEE for periods with valid observations was 0. Unless noted otherwise, all parenthetically

Table 2. Monthly, 24-Hour Averages of Precipitation (P), Sensible Heat Flux (H), Evapotranspiration (ET), Net Radiation (Rn), Temperature (T), Net Ecosystem Exchange (NEE), Gross Primary Production (GPP), and Ecosystem Respiration (R)[a]

Year	Month	P, mm day^{-1}	H, W m^{-2}	ET, mm day^{-1}	R_n, mm day^{-1}	T, °C	NEE, μmol m^{-2} s^{-1}	GPP, μmol m^{-2} s^{-1}	R, μmol m^{-2} s^{-1}
2002	Jan	10.4	20.4	2.43	4.09	25.0	2.7	7.0	9.9
2002	Feb	9.1	17.0	3.2	3.98	25.1	2.2	7.8	10.2
2002	Mar	11.8	16.1	2.71	4.12	24.7	2.2	8.0	10.3
2002	Apr	17.1	21.0	2.98	4.39	24.7	1.7	7.5	9.5
2002	May	6.3	18.0	2.84	4.42	25.7	1.5	7.2	8.8
2002	Jun	3.3	18.8	3.04	4.6	25.3	1.4	6.5	8.0
2002	Jul	2.0	26.8	3.06	5.07	26.1	1.8	6.5	8.4
2002	Aug	0.3	31.9	3.2	5.63	26.6	1.0	7.1	8.2
2002	Sep	0.5	33.6	3.6	6.08	27.1	0.2	7.4	7.7
2002	Oct	0.7	24.7	3.59	5.89	27.0	−1.1	8.4	7.5
2002	Nov	5.4	18.4	3.2	4.27	26.7	0.1	8.1	8.4
2002	Dec	3.0	12.1	3.03	4.26	26.1	0.7	8.1	9.1
2003	Jan	0.9	21.1	2.96	4.79	26.4	−0.5	7.9	7.6
2003	Feb	8.4	14.2	2.4	3.91	24.7	1.0	7.9	9.1
2003	Mar	9.6	15.8	2.61	4.25	24.8	1.5	7.8	9.6
2003	Apr	8.1	19.8	2.75	4.74	25.0	1.4	7.5	9.1
2003	May	8.1	19.2	2.72	4.68	25.3	1.8	7.1	9.1
2003	Jun	5.1	20.0	2.73	4.53	25.3	2.3	6.6	9.0
2003	Jul	2.1	24.7	3.13	4.54	26.0	1.7	6.4	8.2
2003	Aug	2.3	22.8	3.1	5.03	26.4	1.3	6.4	7.7
2003	Sep	3.3	23.9	3.6	5.55	26.6	0.3	8.6	9.0
2003	Oct	1.7	20.7	3.43	5.11	26.7	−0.2	9.0	8.9
2003	Nov	4.9	15.9	3.63	4.7	26.6	−0.3	8.5	8.4
2003	Dec	3.0	12.4	3.62	4.75	26.6	−0.7	8.1	7.7
2004	Jan	13.7	17.0	3.19	4.42	26.0	0.9	7.4	8.5
2004	Feb	15.7	16.1	2.81	4.06	24.6	1.3	8.0	9.5
2004	Mar	8.5	14.1	2.94	4.4	24.9	1.0	8.2	9.4
2004	Apr	9.9	16.4	2.73	4.2	25.2	1.3	8.4	9.9
2004	May	10.3	16.6	2.65	4.16	25.6	1.7	7.7	9.5
2004	Jun	3.1	22.8	3.16	4.62	25.6	1.5	7.4	9.0
2004	Jul	4.9	21.0	3.12	4.92	25.7	1.2	7.2	8.5
2004	Aug	2.3	24.3	3.31	5.34	26.3	1.0	6.9	8.0
2004	Sep	3.3	21.7	3.37	5.38	26.7	−0.2	7.9	7.8
2004	Oct	2.2	23.4	3.52	5.13	27.0	−0.9	8.1	7.3
2004	Nov	0.8	19.1	3.42	4.44	27.7	−1.6	7.5	6.0
2004	Dec	2.0	19.3	3.04	3.47	27.4	−1.3	8.0	6.7
2005	Jan	7.8	21.1	2.77	4.41	27.0	0.3	7.7	8.2
2005	Feb	8.8	18.1	2.54	3.42	25.3	1.6	7.9	9.6
2005	Mar	9.8	21.1	2.8	4.31	25.5	0.3	8.9	9.4
2005	Apr	13.0	21.4	2.67	4.44	25.5	1.5	8.4	10.0
2005	May	9.0	16.8	2.62	4.4	25.3	1.7	7.2	8.9
2005	Jun	3.3	20.2	3.21	4.45	26.1	1.6	6.9	8.6
2005	Jul	1.6	25.0	3.19	4.81	26.3	1.4	6.7	8.2
2005	Aug	1.3	28.1	3.76	5.22	27.1	1.2	6.4	7.7
2005	Sep	1.3	27.2	3.73	5.69	27.1	−0.8	8.2	7.5
2005	Oct	1.8	24.9	3.95	5.77	27.5	−2.2	8.5	6.5
2005	Nov	4.2	21.8	3.29	4.9	27.4	−0.4	8.9	8.6
2005	Dec	10.9	15.8	2.43	3.43	25.2	2.0	7.6	9.7
2006	Jan	9.2	19.8	2.57	3.12	25.3	1.2	8.2	9.6

[a]Data gaps have been filled, see text for details.

reported errors are 95% confidence intervals calculated by bootstrapping the error distributions during similar (e.g., season, hour, PAR level) time periods [*Richardson and Hollinger*, 2005]. Seasonal mean results are based on the mean dry season interval extending from July 15–December 15 with the remainder of the year being considered the wet season.

3. Results

3.1. Weather and Climate

[23] Tables 2 and 3 provide the observed monthly and seasonal mean climatic conditions, energy fluxes, GPP, R, and NEE for the study period from January 2002 through January 2006. The TNF averages 1920 mm per year of precipitation with a mean dry season of 5 months duration (months with <100 mm precipitation), typically extending from July 15 to December 15 [*Parrotta et al.*, 1995]. This site is in the 27th percentile (±2–3%) for both annual precipitation and length of the wet season in the Amazon basin [*Saleska et al.*, 2003; auxiliary material]. There is a regional minimum in annual precipitation in the North-Central Amazon, the location of the TNF, because the propagating sea-breeze front that provides an important trigger for convective precipitation arrives at night [*Garstang et al.*, 1994; *Mitchell et al.*, 2003]. There was also a tendency for precipitation to occur in the late afternoon (1300–1500, local time (LT)) during all seasons,

Table 3. Seasonal Mean Net Ecosystem Exchange (NEE), Gross Primary Production (GPP), Ecosystem Respiration (R), Temperature (T) at 57.8 m, and Cumulative Precipitation (P)[a]

	NEE, kg C ha^{-1} $season^{-1}$	GPP, kg C ha^{-1} $season^{-1}$	R, kg C ha^{-1} $season^{-1}$	T, °C	P, mm $season^{-1}$
Wet 2002	2,893 ± 376	17,550 ± 244	20,443 ± 493	25.2	1,833
Dry 2002	−217 ± 287	12,998 ± 194	12,781 ± 333	26.7	279
Wet 2003	1,376 ± 400	18,079 ± 254	19,455 ± 494	25.3	1,316
Dry 2003	−470 ± 275	13,632 ± 170	13,162 ± 353	26.5	424
Wet 2004	1,194 ± 390	18,924 ± 252	20,118 ± 455	25.4	1904
Dry 2004	−1,416 ± 274	13,023 ± 166	11,607 ± 382	26.8	407
Wet 2005	1,489 ± 356	18,640 ± 234	20,128 ± 545	25.6	1,818
Dry 2005	−1097 ± 262	13,415 ± 174	12,318 ± 353	27.0	383

[a]The dry season extends from July 15–December 15, and the fluxes reported are the seasonal sums for NEE, GPP, R, and precipitation.

due to convective activity stimulated by surface heating. Climatic conditions during our four years of observation were sufficiently variable to allow us to examine both seasonal and inter-annual variability, but did not include major climatic extremes or significant El Niño events.

[24] Meteorology in the TNF is characterized by persistent trade winds [*Lu et al.*, 2005]. Winds at the top of the tower (64 m) were predominantly from the east and northeast. During the afternoons, a westerly river breeze sometimes developed due to differential heating between the forest and the Tapajós River. The river breeze circulation was strongest during hot dry season afternoons, but was also present during dry afternoons in the rainy season. River breezes on average lasted 1.7 hours and developed during approximately 28% of the days.

[25] The mean daily (24-hour average) wind speed recorded at the top of tower by the sonic anemometer was 2.1 ± 0.01 m s^{-1} during the wet season and 2.2 ± 0.01 m s^{-1} during the dry season. The mean daytime (0700–1500, LT) u* was 0.42 ± 0.004 and 0.44 ± 0.006 m s^{-1} during the wet and dry seasons, respectively. The mean nighttime (2300–0500, LT) u* was 0.21 ± 0.004 m s^{-1} for both the wet and dry seasons.

[26] Observed net radiation flux (Rn) and temperature were higher during the dry season (Tables 2 and 3, Figures 2 and 3). Latent heat flux (LE) and vapor pressure deficit (VPD) closely followed the diel patterns in Rn and temperature. During the study period, the daily mean temperature was 25.9 ± 0.74°C, with mean daily minimum and maximum temperatures of 23.5 ± 0.05°C and 29.0 ± 0.08°C, respectively. Air temperature did not follow a symmetric diurnal cycle. Heating was rapid after sunrise (0600 local time), with slow cooling in the afternoon after 1300 (LT). The observed mean RH and mixing ratio of water vapor were 78.2 ± 0.1 % and 16.2 ± 0.07 g H_2O kg dry air^{-1} over the study period, respectively.

3.2. Energy Balance

[27] Net radiation flux (Rn) at the surface can be partitioned into ground heat flux (G), changes in biomass and canopy air heat content (S), atmospheric sensible (H) and

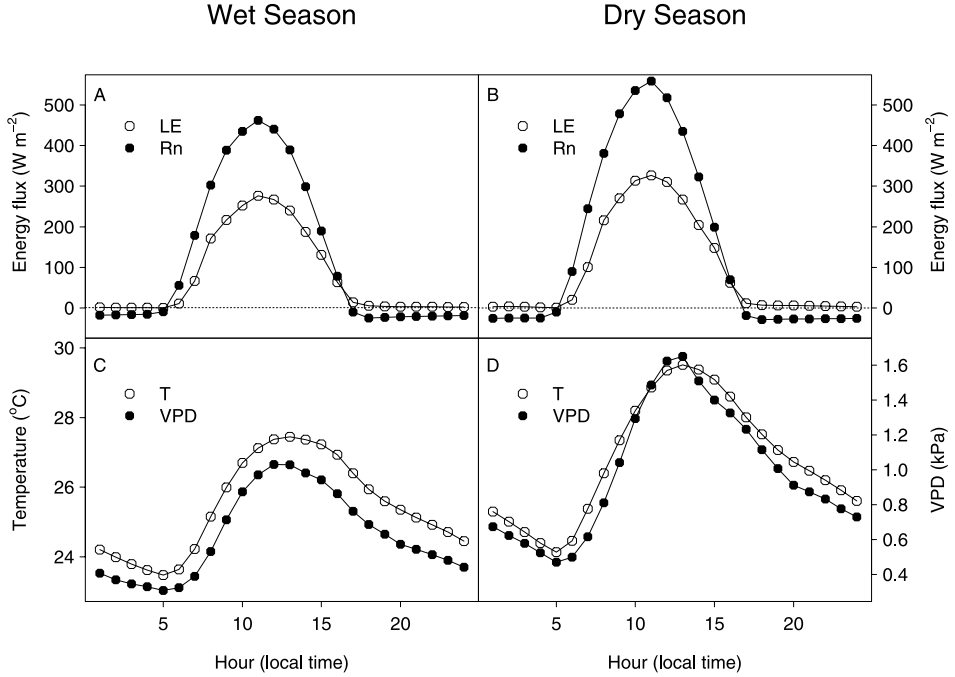

Figure 2. The mean diel cycles of (a) wet season net radiation (Rn, solid circles) and latent heat flux (LE, open circles), (b) dry season Rn (solid circles) and LE (open circles), (c) wet season temperature (T, solid circles) and vapor pressure deficit (VPD, open circles), and (d) dry season T (solid circles) and VPD (open circles).

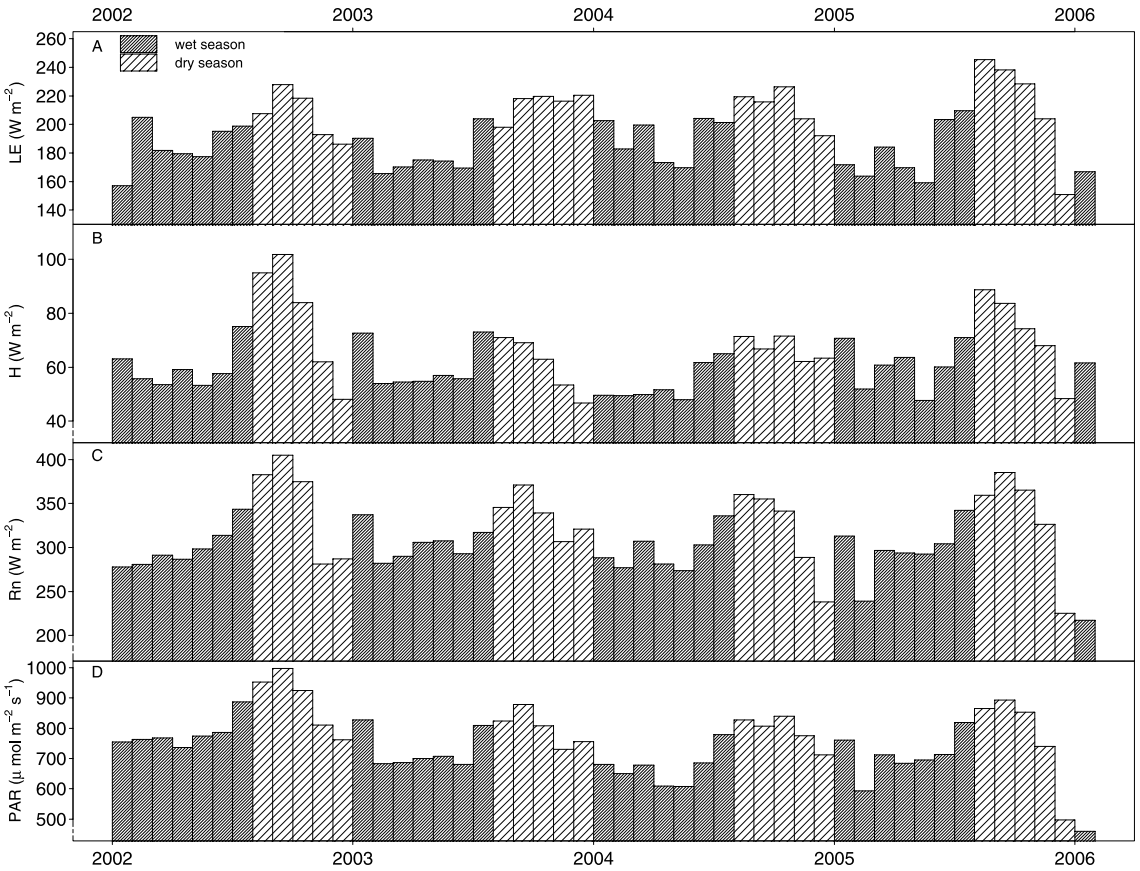

Figure 3. Monthly time series (49 months) of mean daytime (a) latent heat flux (LE, W m^{-2}), (b) sensible heat flux (H, W m^{-2}), (c) net radiation (Rn W m^{-2}), and (d) photosynthetically active radiation (PAR, μmol m^{-2} s^{-1}). The shading patterns within the bars indicate the season.

latent heat (LE) fluxes, and net energy exchange due to precipitation inputs (ΔE_p, see below). Energy balance closure dictates that the sum of LE and H be equivalent to other energy sources and sinks such that

$$Rn - G - S = LE + H + \Delta E_p. \quad (4)$$

Energy balance closure is an important criterion used to assess the reliability and accuracy of surface flux measurements. G was not measured at this site, but has been estimated to be of order 3 W m^{-2} during the daytime (N. Hasler and R. Avissar, What controls Amazon evapotranspiration?, submitted to *Journal of Hydrometeorology*, 2007, hereinafter referred to as Hasler and Avissar, submitted manuscript, 2007) with its 24-hour integral approaching 0. In Amazonian ecosystems, where the quantity of biomass is very large, S has been estimated to be approximately 5–10% of incoming net radiation [*Moore and Fisch*, 1986], but also averages to 0 over daily intervals. S was estimated for this site using the empirical relationship reported in *Moore and Fisch* [1986] for a tropical forest near Manaus, Brazil.

[28] To assess energy balance closure, we examined the slope of an orthogonal distance regression of daytime hourly turbulent heat fluxes (LE + H) versus the total available energy (Rn − S) for all daytime hourly measurements (neglecting ground and ΔE_p fluxes); average closure was 85% (±0.08) using this method. Energy closure was higher during the dry season (88 ± 0.1%) than the wet season (83 ± 0.08%). The seasonal closure difference may be a measure of unquantified heat exchanged by precipitation. For example, a 10 mm hr^{-1} rain event, with the water ten degrees cooler than ambient air, could result in an apparent loss of 116 W m^{-2} from the ecosystem that is not captured in this analysis. On an annual basis the energy flux due to rain (~2000 mm yr^{-1}) is of order 3% of the total net radiation, and will have a larger impact in the wet season. Measurement artifacts such as sensor separation and finite volume averaging also result in small, consistent losses in LE and H fluxes [*Finnigan*, 2004]. Given the overall consistency between wet and dry energy closure results, there is no reason to suspect our fluxes are significantly biased on seasonal timescales. Our observed 15% lack of closure in hourly data is similar to observations at most flux tower sites; global average closure was found to be 79% [*Wilson et al.*, 2002] and 82% within the Amazon tower sites (Hasler and Avissar, submitted manuscript, 2007). The slope of the 24-hour energy closure (LE + H vs. Rn) was 93% (±2.8), using only days with complete data coverage (more common in the wet season).

3.3. Ecosystem Carbon Fluxes

[29] The annual (January–December) carbon balances at this site were 2677 ± 488, 906 ± 491, −221 ± 453, and 392 ± 449 kg C ha^{-1} yr^{-1}, for 2002–2005, respectively, indicating a small net source of carbon to the atmosphere over the period, declining to approximate carbon balance over four

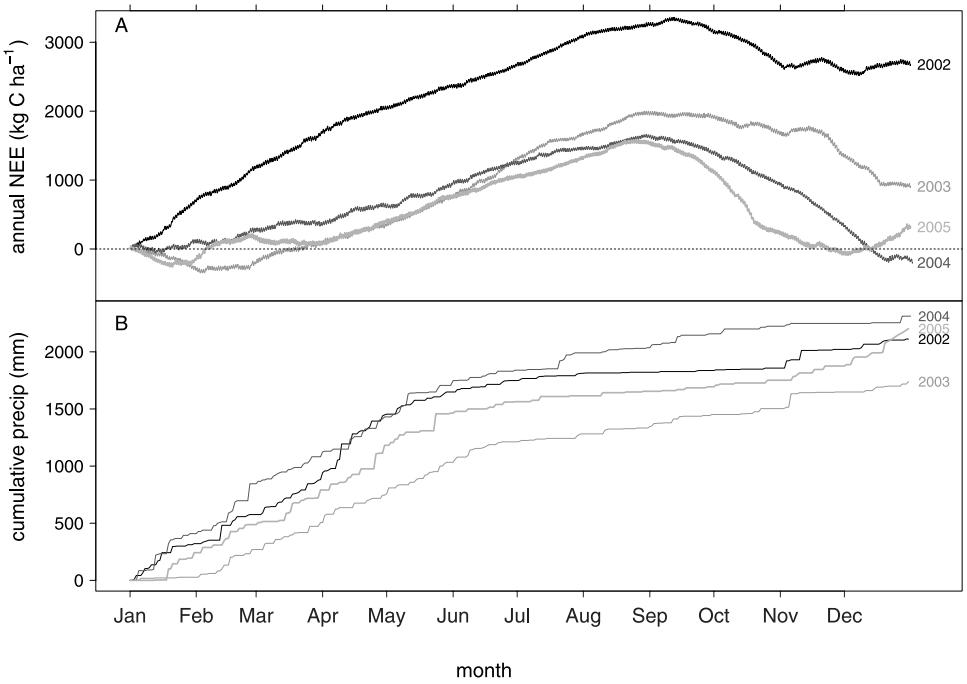

Figure 4. Time series of (a) cumulative net ecosystem exchange of CO_2 (annual NEE, kg C ha^{-1}) for January 1, 2002–January 19, 2006 and (b) cumulative precipitation (mm).

years. The complete record analyzed here confirms the seasonal patterns initially reported for the TNF by *Goulden et al.* [2004] and *Saleska et al.* [2003]. During the wet season R was generally greater than GPP, resulting in a net carbon loss to the atmosphere (Tables 2 and 3, Figures 4 and 5). During the dry season the reverse was more common, with GPP exceeding R resulting in net carbon uptake from the atmosphere.

[30] The mean annual ecosystem respiration was 8.6 ± 0.11 μmol m^{-2} s^{-1}, with a mean of 9.2 ± 0.15 and 7.7 ± 0.15 μmol m^{-2} s^{-1} for the wet and dry seasons, respectively. Maximum respiration was observed during the mid-wet season in March and minimum respiration was observed during the late dry season in October (Table 2 and Figure 5). The mean annual GPP was 8.3 ± 0.11 μmol m^{-2} s^{-1} with no statistically significant seasonal difference in carbon uptake, 2614 ± 93 kg C ha^{-1} month^{-1} and 2653 ± 79 kg C ha^{-1} month^{-1} for the wet and dry seasons, respectively.

[31] The total ecosystem R was lower during the dry season, but the decline in R typically began during the latter part of the wet season, in synchrony with the decline in the canopy carbon uptake. R tended to remain low throughout the dry season even as canopy uptake increased. This observation appears to highlight differential responses of the autotrophic and heterotrophic components of R. Autotrophic R can be assumed to increase with increasing GPP. Hence, reduction of R in the dry season is very likely to represent moisture limitations on heterotrophic R. Over four years, the TNF was a source of carbon to the atmosphere with an observed mean loss of 890 ± 220 kg C ha^{-1} yr^{-1}.

3.4. Ecosystem Water Fluxes

[32] Observed ET ranged widely, from 0.67 to 6.24 mm day^{-1}, with average rates of 2.89 ± 0.15 and 3.41 ± 0.18 mm day^{-1} for the wet and dry seasons, respectively. The annual mean total was 1135 mm. Across the four measurement years, ET consistently increased at the start of the dry season and remained elevated throughout the entire dry season (Figure 3). ET rates were within the range observed at other Amazonian flux sites (see Amazon-wide comparisons in *Hutyra et al.* [2005]), but the data were significantly lower than modeled ET reported by *Nepstad et al.* [2004] and *Lee et al.* [2005]. The annual fraction of precipitation lost through ET was fairly constant during the study period at 0.53 (1116 mm/2111 mm), 0.64 (1114 mm/1740 mm), 0.49 (1137 mm/2311 mm), 0.51 (1123/2201) for 2002–2005, respectively. The ratios of evaporation to precipitation during the dry seasons of 2002, 2003, 2004, and 2005 were 1.81 (503.3 mm/278.5 mm), 1.16 (521.8 mm/448 mm), 1.28 (514.4 mm/402.4 mm), and 1.40 (535.7 mm/382.9 mm), respectively. Dry season ET was insensitive to dry season precipitation, being nearly constant across years even though dry season precipitation varied by 40%.

[33] There was no statistically significant difference observed between the wet and dry seasons in the slope of LE and H versus Rn (Figure 6). The mean annual evaporative fraction (LE/Rn) was 0.62. This invariance contrasts markedly with data reported by *Malhi et al.* [1998, 2002], who observed significant seasonal differences in the evaporative fraction in an Amazonian forest near Manaus, Brazil, that actually receives more rainfall and has a shorter dry period. The observed patterns are consistent with the findings of *da Rocha et al.* [2004] for the nearby tower at km 83.

3.5. Independent Estimates of Carbon Flux

[34] It is critical to independently validate carbon flux measurements in order to ensure accurate cumulative sums and to examine the mechanisms controlling exchange. Biases in day/night measurements of CO_2 flux could

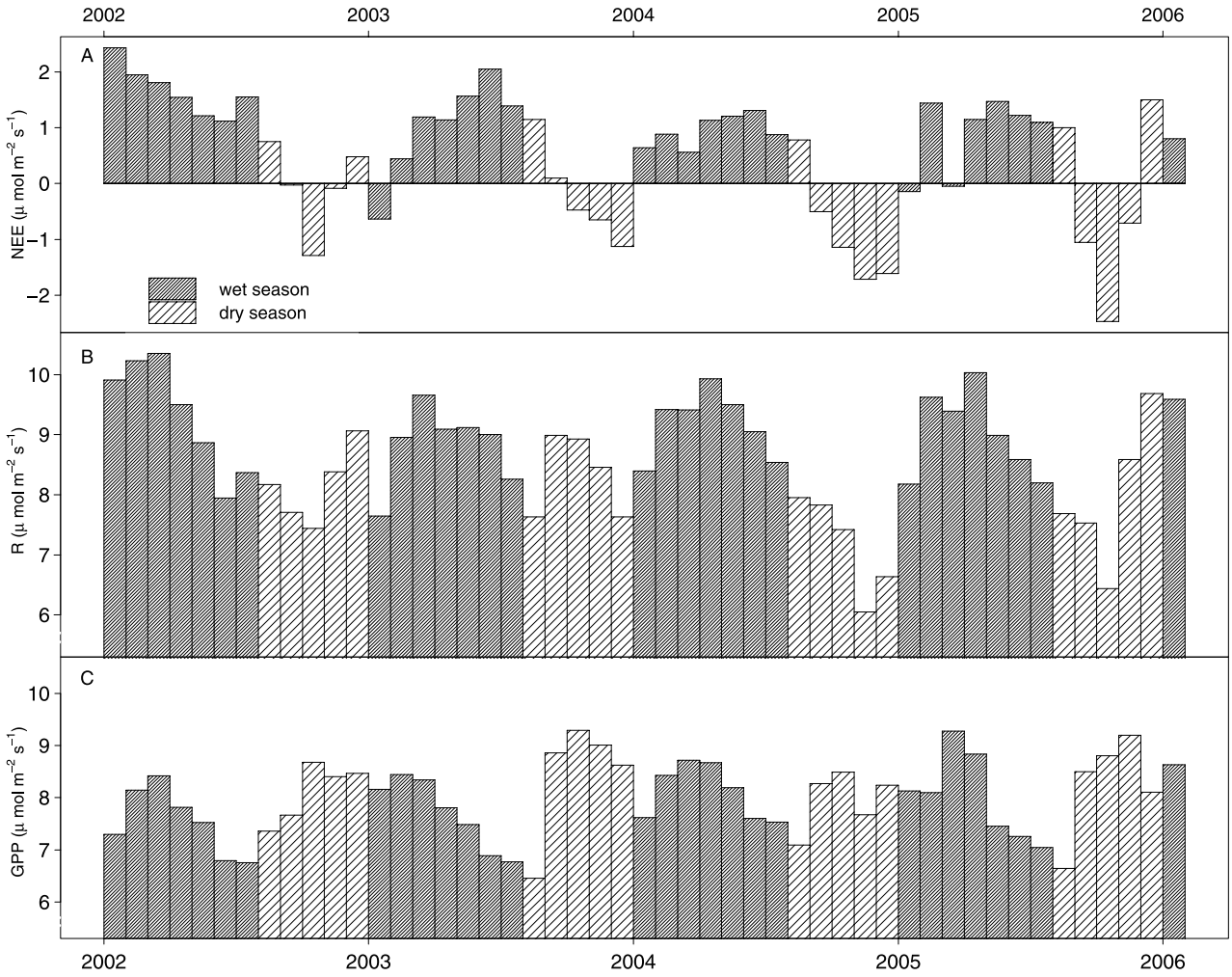

Figure 5. Monthly time series (49 months) of (a) net ecosystem exchange of CO_2 (NEE, μmol m^{-2} s^{-1}), (b) ecosystem respiration (R, μmol m^{-2} s^{-1}), and (c) gross primary production (GPP, μmol m^{-2} s^{-1}). The shading patterns within the bars indicate the season.

significantly affect estimates of the overall carbon balance. A potential source of bias is the prevalence of weak vertical mixing during the nighttime hours, leading to a violation of the assumption of horizontal homogeneity required for eddy flux measurements and to 'lost flux' associated with horizontal advection [*Finnigan*, 2004]. We used three independent approaches to ensure unbiased data for nighttime fluxes and to validate flux measurements: (1) filtering the data according to u* values to correct for underestimation of nighttime fluxes; (2) analysis of annual and seasonal light response relationships between PAR and NEE to derive independent estimates of nighttime NEE, avoiding any use of nighttime data or u* filtering; (3) estimation of nighttime NEE by similarity of CO_2 with ^{222}Rn.

[35] 1. Respiration is a biological process that should be largely independent of the turbulence intensity. Since measured NEE decreased in calm conditions (Figure S2), there appears to be some lost flux. Approximately 57% of the nighttime hours at this site were calm, with u* < 0.22 m s^{-1}. We corrected for lost flux by filtering calm night periods and replacing the data with the mean value for proximate well-mixed time periods (defined as u* $\geq$ 0.22 m s^{-1}, see *Saleska et al.* [2003] and Hutyra et al. (submitted manuscript, 2007) for further discussion of u* corrections and the relationship between canopy CO_2 storage and turbulence). Note that the prevalence of strong turbulence (high u*) in both daytime and nighttime is higher at the TNF than observed at many Amazonian flux towers, giving better mixing and fewer gaps in the nighttime flux [cf. *Kruijt et al.*, 2004]. The observed mean nighttime NEE with u* filtering was 9.2 ± 0.15 and 7.7 ± 0.15 μmol m^{-2} s^{-1} for the wet and dry seasons, respectively; were no u* filter applied the respective mean nighttime NEE would be 7.1 ± 0.09 and 5.8 ± 0.10 μmol m^{-2} s^{-1}.

[36] 2. We examined NEE-light relationships (Figure 7) using a nonlinear least squares approximation (hyperbolic function)

$$NEE = a_1 + \frac{a_2 \times PAR}{a_3 + PAR} \quad (5)$$

fitted to NEE and PAR. We excluded data for PAR $\leq$ 40 μmol m^{-2} s^{-1}, since these data points often correspond to periods of low turbulence and rapidly changing light levels, resulting in large uncertainties. The intercept, a_1, of this fit provides an independent estimate of mean ecosystem R (limit of equation (5) as PAR $\rightarrow$ 0). The annual mean value

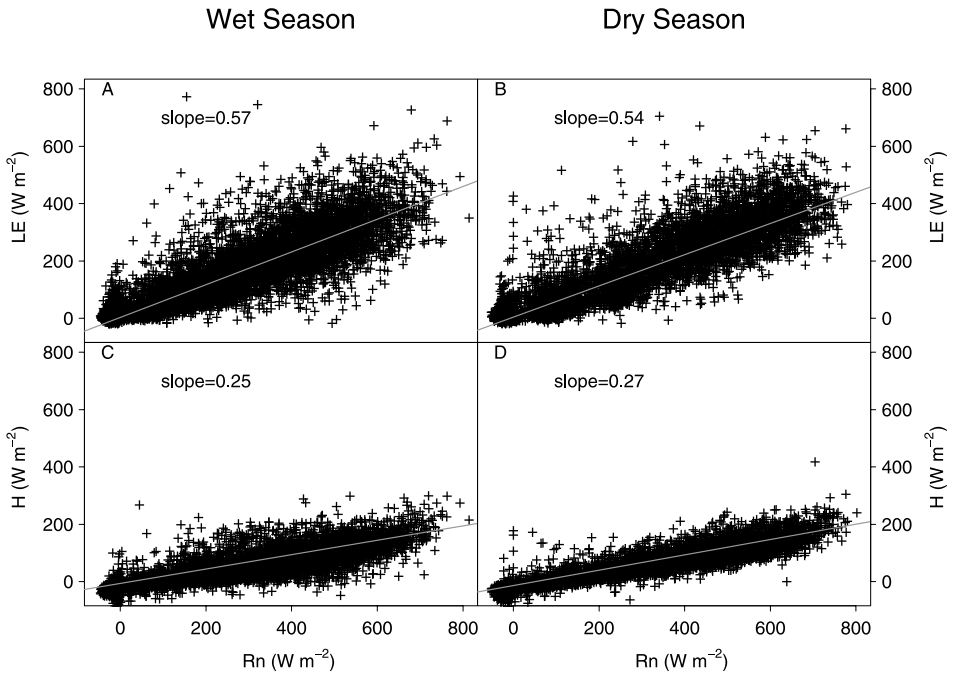

Figure 6. (a) Hourly latent heat flux (LE, W m^{-2}) as a function of net radiation (W m^{-2}) during the wet season. (b) Hourly LE as a function of net radiation during the dry season. (c) Hourly sensible heat flux (H, W m^{-2}) as a function of net radiation during the wet season. (d) Hourly H as a function of net radiation during the dry season. The slope reported is from an orthogonal distance regression.

of a_1 was 8.9 ± 0.6 μmol m^{-2} s^{-1}, based on all available data (no u* filter applied), and statistically indistinguishable from the mean nighttime u* filtered NEE (8.6 ± 0.13 μmol m^{-2} s^{-1}). Note that the respective data sets are completely disjoint. Seasonal comparisons between a_1 and u*-filtered mean nighttime NEE also agreed within 5% (Figure S3).

[37] 3. Data for ^{222}Rn can potentially define rates of forest-atmosphere exchange, since ^{222}Rn is conserved after emission from the soil (apart from slow radioactive decay). *Martens et al.* [2004] independently assessed raw and u* corrected eddy flux NEE measurements at night by comparing CO_2 eddy flux data with CO_2 fluxes inferred from ^{222}Rn profiles and ^{222}Rn soil flux measurements. Nighttime NEE derived from ^{222}Rn was found to be 9.0 ± 0.99 μmol m^{-2} s^{-1} for the wet season (June–July 2001) and 6.4 ± 0.59 μmol m^{-2} s^{-1} in the dry season (November–December 2001), agreeing very well with u* filtered NEE measurements during the same period (8.65 ± 1.07 and 6.56 ± 0.73, respectively) [*Martens et al.*, 2004].

[38] The independent light-curve and ^{222}Rn based estimates of nighttime NEE both agree extremely well with the u*-filtered nighttime flux measurements. Failing to apply a u* filter to the data would have changed the annual sum of carbon exchange from a small carbon source to a significant carbon sink, almost 10 Mg C ha^{-1} yr^{-1}. This value would also markedly disagree with bottom-up estimates for this site [*Rice et al.*, 2004; *Saleska et al.*, 2003; Hutyra et al., submitted manuscript, 2007].

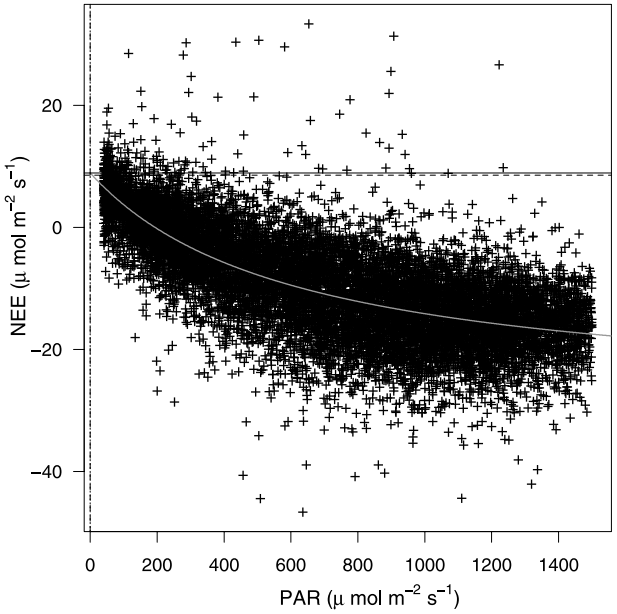

Figure 7. Net ecosystem exchange of CO_2 (NEE, μmol m^{-2} s^{-1}) as a function of photosynthetically active radiation (PAR, μmol m^{-2} s^{-1}). A nonlinear least squares approximation (hyperbolic function) is plotted through the data. The vertical line denotes 0 μmol m^{-2} s^{-1} PAR. The dashed horizontal line is the mean nighttime NEE (8.6 ± 0.1 μmol m^{-2} s^{-1}, u* $\geq$ 0.22). The solid horizontal line is the a_1 intercept term from the hyperbolic fit (equation (5)) estimating of mean nighttime respiration (8.9 ± 0.6 μmol m^{-2} s^{-1}).

4. Discussion

4.1. Controls on NEE

[39] The carbon balance of an ecosystem is the result of disturbance and recovery dynamics over timescales of years

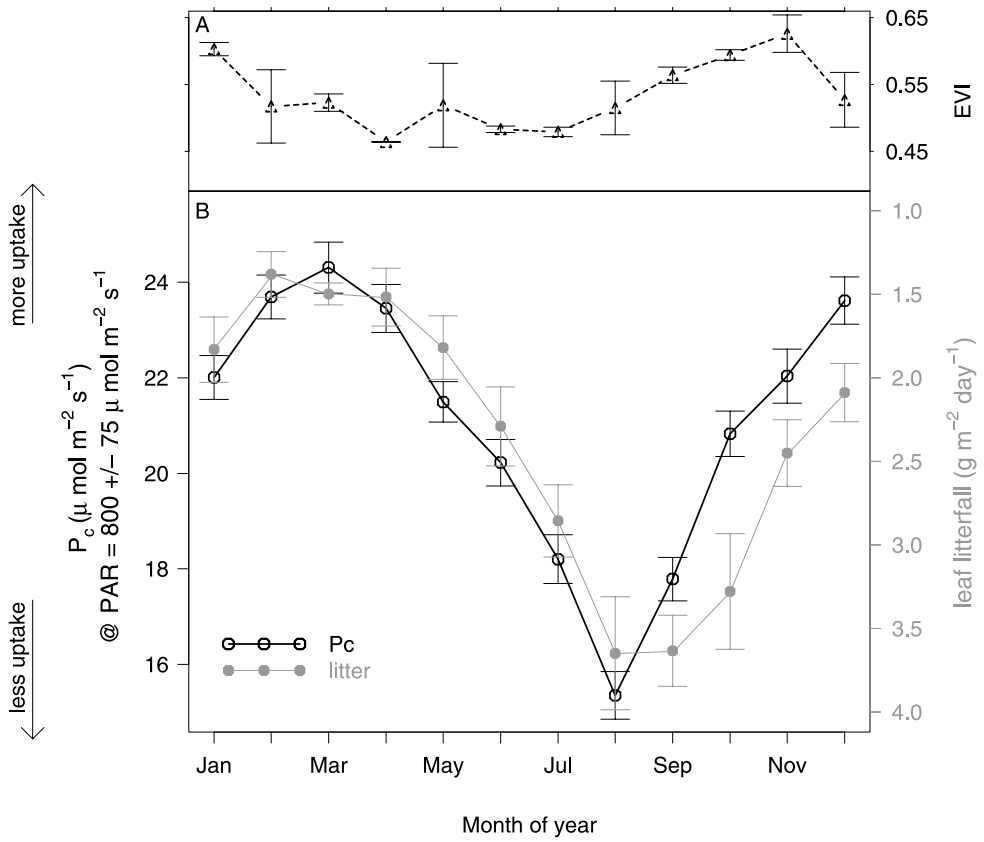

Figure 8. (a) Monthly mean Enhanced Vegetation Index (EVI), 2000^{-2}005, triangles [*Huete et al.*, 2006]. (b) The forest canopy efficiency is expressed as the monthly mean gross primary production (GPP) where photosynthetically active radiation is 725–875 μmol m^{-2} s^{-1}, open circles. Monthly mean leaf litterfall rate, July 2000–May 2005, solid circles (see *Rice et al.* [2004] for methodological details). The error bars denote standard error. Note that the axis for litterfall is inverted to highlight the correlation with P_c.

and decades [*Saleska et al.*, 2003; *Rice et al.*, 2004; *Vieira et al.*, 2004], upon which is superimposed the influence of weather anomalies on seasonal and annual timescales. Figure 4 shows the cumulative annual cycles of NEE, highlighting the dominance of ecosystem respiration throughout the early portion of the calendar year (wet season) as the forest lost carbon to the atmosphere. By September, increases in canopy uptake generally began to dominate and the forest turned into a carbon sink for the rest of the dry season. The transition back to a net carbon source followed the arrival of wetter weather.

[40] Climate anomalies exerted strong control on the inter-annual variations in net carbon balance. In 2005, carbon losses in the wet season were relatively small and the transition to carbon uptake was very abrupt, and by November the year was on track to be a significant carbon sink. But, the early arrival of the wet season, with significant November and December rainfall, reversed the carbon uptake and the site was instead an overall carbon source in 2005 (Figures 4 and 5). In January 2003, low precipitation, totaling only 27 mm, resulted in reduced respiration rates. However, GPP rates remained high, leading to a carbon sink for the month despite the seasonal norm (Figures 4 and 5). The greatest variability in monthly total NEE was observed during the late dry season and early wet season (November–January). Respiration rates were the most variable and sensitive to precipitation and temperature anomalies (Figure 5).

4.2. Controls on Gross Primary Production

[41] Many process-based biogeochemical models [e.g., *Botta et al.*, 2002; *Tian et al.*, 1998] predict that moisture limitation during the dry season should provide a strong constraint on canopy carbon uptake in tropical forests like the TNF. Four years of observations at the TNF do not support this paradigm. Uptake was indeed reduced early in the dry season, but the decline began before the onset of the dry weather. Moreover, uptake started to increase in the driest period, well before the onset of the rainy season (Table 2; Figures 4 and 5). The forest maintained high rates of photosynthesis throughout the year because of adequate water supplies, high year-round temperatures, and high light levels. *Goulden et al.* [2004] observed a similar seasonal pattern in photosynthesis at a nearby forest site between July 2000 and July 2001.

[42] Peak litterfall rates were observed at the TNF in August [*Rice et al.*, 2004], early in the dry season, and the flush of new leaves across the Basin also occurred in the dry season, August–October (Figure 8) [*Huete et al.*, 2006; *Rivera et al.*, 2002]. Younger leaves have higher photosynthetic efficiency [*Freeland*, 1952] and hence it is not

Table 4. Summary of Explained Variance (R^2) and Best Regression Equations Used to Estimate Ecosystem Respiration (R) as a Function of Mean Daily Maximum Temperature (T, °C) and Cumulative Precipitation (P, mm)

	$\overline{T}_{dailymax}$, °C	$\sum P$, mm	$\overline{T}_{dailymax}$ and $\sum P$	Best Model
Hourly timescale	-	-	-	-
Daily timescale	0.05	-	-	-
Weekly timescale	0.12	0.06	-	-
14-day timescale	0.29	0.24	0.32	$R = 22.9 - 0.51*T_{max} + 0.05*P$
21-day timescale	0.45	0.32	0.47	$R = 25.1 - 0.58*T_{max} + 0.03*P$
Monthly timescale	0.67	0.54	0.72	$R = 26.1 - 0.62*T_{max} + 0.03*P$
Seasonal timescale	0.92	0.45	0.92	$R = 39.9 - 1.1*T_{max}$

surprising that higher rates of GPP were observed in the months following leaf-out in the dry season. Previous work by *Wright and van Schaik* [1994] also showed that tropical plants produce new leaves when irradiance is maximized.

[43] To quantify the phenology effects on GPP at this site, we calculated "canopy photosynthetic capacity" (P_c) as the mean monthly GPP in a fixed light interval (PAR 725–875 μmol m^{-2} s^{-1}), and compared the time series of this quantity with leaf litterfall rates and with remotely sensed vegetation greenness (enhanced vegetation index, EVI) at the TNF [*Huete et al.*, 2006]. We examined Pc to remove the influence of seasonal differences in incoming radiation. Figure 8 shows that leaf litterfall rates were strongly correlated with P_c ($r^2 = 0.76$ or 0.83, for lags of 0 or 1 months, respectively). In contrast, EVI correlated weakly with P_c, explaining at best only 56% of the observed variance with a long lag (3 months). EVI, lagged by 2 months, was somewhat better correlated with monthly litterfall ($r^2 = 0.63$). The temporally lagged correlations in EVI and/or litterfall are not surprising since it takes time for the leaves to fully elongate and develop their pigmentation. Note that total GPP, across all light levels, also correlated with litterfall ($r^2 = 0.63$, lagged by 2 months) and EVI ($r^2 = 0.40$, leading by 1 month).

[44] During the late dry season there are also increased aerosol loadings due to land clearing and agricultural activities, resulting in higher diffuse light levels. P. H. F. Oliveira et al. (The effects of biomass burning aerosols and clouds on the CO_2 flux in Amazonia, submitted to *Tellus, Ser. B*, 2007, hereinafter referred to as Oliveira et al., submitted manuscript, 2007) observed maximum aerosol loading at the TNF between September and November. Higher photosynthetic rates have been observed under diffuse light conditions [*Gu et al.*, 2003; Oliveira et al., submitted manuscript, 2007]. Either or both leaf replacement and aerosol light scattering may account for increased P_c in the late dry season (October–December, Figure 7). There was significant inter-annual variation in both EVI and P_c, see Figure S4 for the full available time series.

4.3. Controls on Ecosystem Respiration

[45] Ecosystem respiration is the sum of CO_2 released by plant leaves, stems, and roots (autotrophic respiration), and CO_2 released through decomposition of organic material (heterotrophic respiration). Temperature and moisture are key environmental factors regulating respiration rates, but the interaction among these parameters is still poorly understood [*Raich and Schlesinger*, 1992; *Trumbore*, 2006]. Temperature and soil moisture are typically inversely correlated, but both factors simultaneously influence R by affecting enzyme activity, diffusion of solutes and O_2, growth of root tissue, and microbial populations [*Davidson et al.*, 2006]. Eddy covariance data cannot distinguish the components of respiration. However, our long data set from the TNF does allow us to examine the aggregate effects of climatic variability on total ecosystem respiration, over timescales from hourly to inter-annual.

[46] Relationships between R and temperature have been reported in many ecosystems, and ecosystem models often use exponential relationships to describe these data, with Q_{10} values typically between 1 and 2 [e.g., *Davidson et al.*, 2006]. But decomposition of organic material in tropical forest soils is known to have a relatively low temperature sensitivity [*Davidson and Janssens*, 2006]. At the TNF, there was no statistically significant relationship between nighttime CO_2 flux and ground or canopy temperature, or precipitation, over any time interval from hourly to weekly (Table 4). *Davidson et al.* [2004], working at nearby site (~5 km), also found no significant relationship between soil volumetric water content and observed soil CO_2 respiration rates using chamber methods. The absence of a significant relationship between temperature and ecosystem R could be an artifact of high mean temperature, with canopy and ground mean temperatures averaging 24.8°C and 24.6°C, respectively, or of the small temperature range seasonally, diurnally, and during the nighttime. It also possible that the entire temperature range is within a broad optimum for this ecosystem or that the temperature responses of multiple processes may cancel when aggregated to the ecosystem scale. The observations imply that models of tropical forests which include an exponential relationship between respiration and temperature may over-predict the temperature sensitivity of respiration rates at the ecosystem level.

[47] When averaged on longer timescales, temperature and precipitation were significant correlates of total ecosystem respiration and a temperature regression could indeed explain the most significant portion of the total observed variance (Table 4). But, respiration was negatively correlated with temperature and positively correlated with precipitation, and the apparent relationship between R and temperature arises because temperature and precipitation are negatively correlated. We examined the intercept values (a_1) of morning versus afternoon light-curve extrapolations (equation (5)) and found no significant difference in the respiration estimates in the dry season, although temperature differences were near their maximum (Figure S5). In contrast, during the wet season we found that morning respiration estimates were higher than the afternoon estimates in three of four observed wet seasons (Figure S5). Higher morning respiration highlights the dominance of

moisture in controlling heterotrophic respirations rates since nighttime precipitation is very common while morning temperatures were lower. We conclude that the negative respiration-temperature correlation is likely a simple artifact that arises because wet seasons, which have higher respiration rates, are cooler than dry seasons.

[48] Maximum litterfall rates (leaves, twigs, and fruits) were observed shortly after the onset of the dry season in August and September (Figure 8) [*Rice et al.*, 2004]. Tropical forest litter typically has a short turnover time (less than 1 year [*Brown and Lugo*, 1982]), but during the dry season, following the peak input of litter, moisture levels are low in soil and litter. Hence, ecosystem respiration rates remain low, even though substrate abundance, temperatures, and canopy metabolic rates were highest in the dry season.

[49] *Chambers et al.* [2004] estimated the mean ecosystem respiration rate to be 7.8 μmol m^{-2} s^{-1} at a site near Manaus, Brazil by measuring individual components of ecosystem respiration, compared to 8.4 μmol m^{-2} s^{-1} (7.5–9.4 95% CI) using eddy covariance method at that site. Using chamber-based methods, *Chambers et al.* [2004] estimated a mean soil respiration rate of 3.2 μmol m^{-2} s^{-1} at the Manaus site and reported that both soil respiration and total ecosystem respiration declined with increasing soil moisture, opposite to our observations. *Chambers et al.* [2004] speculated inadequate oxygen supplies in saturated soils led to lower respiration rates. Soil respiration measured at the TNF (R. K. Varner et al., manuscript in preparation, 2007) averaged 2.63 μmol m^{-2} s^{-1} annually and 2.91 and 2.29 μmol m^{-2} s^{-1} for the wet and dry seasons, respectively, and showed an increase with precipitation and a negative correlation with temperature, in harmony with our data for total ecosystem R. Thus, R at these two sites showed opposite seasonality, peaking during the wet season at the TNF but in the dry season at Manaus.

[50] It is not known why these sites exhibit different seasonality in respiration. The TNF has much more coarse woody debris (CWD; 48 ± 5.2 Mg C ha^{-1} [*Rice et al.*, 2004; G. W. Santoni et al., manuscript in preparation, 2007]) than in Manaus (10.5 Mg C ha^{-1} [*Chambers et al.*, 2000]; 15.7 ± 4.1 Mg C ha^{-1} [*Nascimento and Laurance*, 2004], assuming that 1 kg dry biomass = 0.5 kg C biomass). In the TNF, CWD respiration was estimated to be a very significant component of the overall respiration budget contributing 1.2 ± 0.3 μmol m^{-2} s^{-1} (see Hutyra et al. (submitted manuscript, 2007) for a full breakdown of the TNF respiration budget). In contrast, CWD respiration estimates from Manuas are significantly smaller, contributing only ~0.50 μmol m^{-2} s^{-1} [*Chambers et al.*, 2004]. Seasonal patterns of CWD respiration are very poorly quantified for the tropics, but it is possible that the moisture and temperature responses of CWD respiration could differ significantly from soil R. The combination of a longer dry season and a larger stock of CWD at the TNF may contribute to changes in CWD respiration and help explain the seasonal differences versus Manaus. It is also possible that a different moisture optimum exists in Manaus due to the shorter dry season and greater annual rainfall. Further, topographic and soil differences between the Manaus and TNF sites are likely to also contribute to the opposite seasonal respiration patterns. The Manuas study site is located within an area of undulating topography with often inundated soils in the low-lying areas [*Araújo et al.*, 2002] while the TNF has very little topographic variation, no soil inundation, and an extremely deep water table. The physical reason for the seasonal differences in respiration remains an open question in of need further research.

4.4. Is Forest Growth Water Limited?

[51] Seasonal water limitations have the potential to reduce forest growth and place the forest at risk for fire. Future climate scenarios suggest that temperatures in the Amazon may increase while precipitation decreases [*Fung et al.*, 2005], likely decreasing water availability and increasing drought and flammability. To assess the current sensitivity of this forest to water limitations, we looked at the patterns in water flux, seasonal evaporative balances, water-use efficiencies, and light-use efficiency.

[52] ET rates consistently increased at the start of the dry season and remained elevated throughout the period of maximum radiation inputs (Figures 2 and 3). Water losses consistently exceeded inputs during the dry season, large stores of water are evidently accessible to the trees. In the case of 2002, approximately 225 mm of water was withdrawn from storage during the dry season. If we adapt as representative the plant available water profile measured in a similar soil by *Nepstad et al.* [1994], the forest had to extract water from depths in excess of 4 m to support the observed dry season ET rates. The higher ET rates and the nearly inelastic total ET in the dry season are both strong indicators of adequate water availability at the TNF with the current climate.

[53] Ecosystem water-use efficiency (WUE) can be defined as the ratio of GPP to F_{H2O} (carbon uptake/water loss). Elevated values of WUE could indicate water stress as the scarce resource (water) is conserved. But, the mean observed WUE was 4.5 and 3.7 μmol CO_2/mmol H_2O for the wet and dry season, respectively, showing the opposite trend. Although this result is consistent with this ecosystem not experiencing seasonal water stress, it must be interpreted cautiously. Changes in the WUE can result from a change in either the canopy carbon uptake or F_{H2O}. As the dry season approached, F_{H2O} and the vapor pressure deficit started to increase while the GPP started to decrease, resulting in a lower overall dry season WUE. The WUE started to increase again in October when canopy carbon uptake increased, while the F_{H2O} remained high (Tables 2 and 3).

[54] Both light-use efficiency (LUE) and WUE were significantly higher in the morning than afternoon (Figure 9). The diel patterns in the LUE and WUE are consistent with afternoon GPP being inhibited. The standard paradigm is that as VPD increases, plant water stress will increase and stomatal conductance will decrease, resulting in higher WUE and lower LE and LUE. However, at this site the LE remains high in the afternoon (Figure 2) and the overall evaporative fraction increased along with VPD, likely indicating abundant water supplies. The fraction of water lost through transpiration may change diurnally, but the LE measurements can not be readily separated into the component processes. It is possible that the apparent afternoon reductions in GPP were due to differences in autotrophic respiration rates, but the analysis of light-curve intercepts (Figure S5) does not support that interpretation. The morning and afternoon differences in WUE and LUE are more

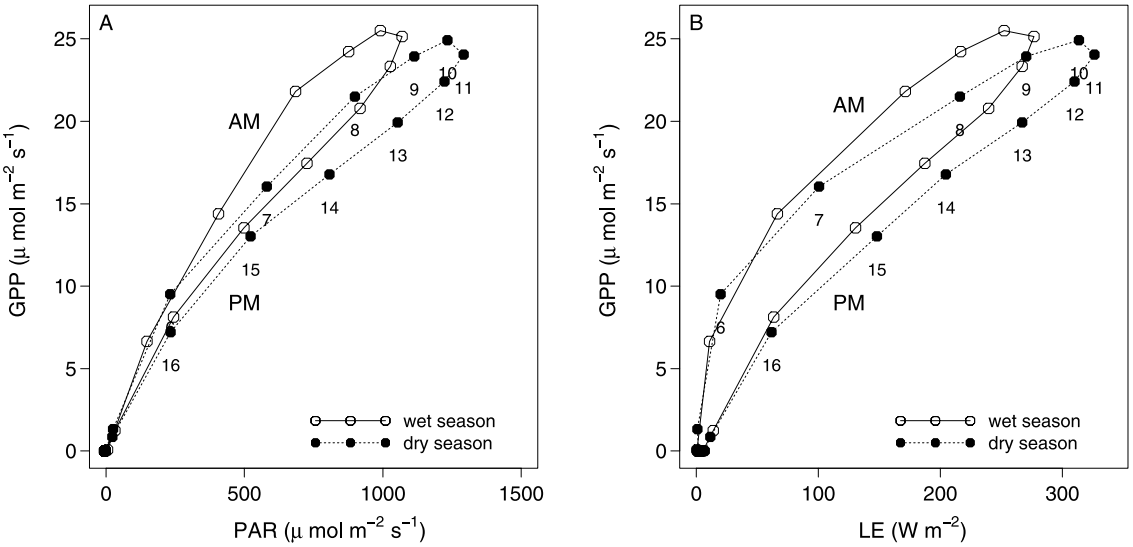

Figure 9. (a) Diel cycles of gross primary production (GPP) as a function of photosynthetically active radiation (PAR) for the wet (open circles) and dry (solid circles) seasons. (b) Diel cycle of GPP as a function of latent heat flux (LE) for the wet (open circles) and dry (solid circles) seasons. The numbers along the curve indicate the local time.

likely due to limitation on stem conductance, plant circadian rhythms [*Doughty et al.*, 2006], metabolic cycles (e.g., respiration associated with sugar transport), or enzymatic limitations.

5. Summary and Conclusions

[55] In this study we critically assessed flux measurements of CO_2 and H_2O and examined energy closure to ensure the validity of the observations, then we examined the controls on carbon and water exchange in an evergreen tropical rain forest. We found no significant signs of water limitation on photosynthesis: trees had adequate water supplies throughout the 5 month dry season. ET responded strongly to radiative drivers year-round and was insensitive to dry season precipitation totals. Observed dry season evaporative losses significantly exceeded precipitation inputs, drawing up to 225 mm of water from water reserves that had to extend many meters in depth. Evidently the annual input of precipitation and the capacity of the plants to use stored water over considerable depth provide the key to maintaining this closed canopy equatorial forest despite long periods of low rainfall.

[56] We found that the seasonal course of canopy photosynthesis was largely controlled by phenology and light. Canopy photosynthetic efficiency declined before leaf senescence (late wet season) and increased after new leaf elongation (mid-dry season). Unfortunately, the EVI parameter did not capture this pattern. Phenological control of the timing of peak carbon uptake capacity (P_c) again highlights adequate water availability and suggests that the assemblage of trees in this forest may have been selected to optimize for light, not water. The dominant influence of phenology versus water stress is a significant surprise for this forest.

[57] Climate anomalies exerted a strong influence on net carbon exchange, principally through effects on R. Ecosystem R was lower during the dry season due to moisture limitations on heterotrophic respiration as evidenced by enhanced dry season GPP and Pc rates. We did not find a significant relationship between temperature and R on short timescales. The lack of temperature dependence raises uncertainty about the appropriateness of using Q-10 type relationships in ecosystem models of tropical rain forests. The largest variations in R, photosynthesis, and net carbon exchange were observed during the dry-to-wet season transition.

[58] This forest currently does not exhibit signs of water limitations, with enough water to satisfy growth requirements. It was a small overall carbon source to the atmosphere, with the efflux rate declining over the period of study, consistent with the long-term ecosystem disturbance and recovery dynamics as proposed by *Rice et al.* [2004] and with the large contribution of CWD respiration to the observed high rates of respiratory carbon losses. Live biomass stocks have increased significantly over the study period while CWD stocks have decreased (G. W. Santoni et al., manuscript in preparation, 2007).

[59] If precipitation rates were to decrease by a small amount, but water supplies remained adequate for the trees, it is possible that the net carbon uptake could increase due to higher insolation and slower heterotrophic respiration. However, a reduction in decomposition from drier conditions could result in increased flammability due to a build up of fuel. Alternatively, if the amount of available water for the trees were to decrease through logging (causing soil compaction), higher temperatures (increasing the evaporative demands), or large decreases in precipitation (slowing recharge of deep water reservoirs) the flammability of this forest might increase and the forest may convert to a fire adapted vegetation type. Accurate predictions of future climate and land-use changes require capturing these critical dependencies on precipitation and on ecosystem structure and function.

[60] **Acknowledgments.** Thanks to David Fitzjarrald and the SUNY Albany team for providing weather station data which were critical for gap filling. The authors would like to thank Paul Moorcroft and Michael Keller's entire team for insightful comments and suggestions throughout this project. We thank Elizabeth Hammond-Pyle, Amy Rice, Alfram Bright, John Budney, and Daniel Curran for their engineering and field assistance; Bethany Reed, Lisa Merry, Dan Hodkinson, Fernando Alves Leao, and the staff of the LBA Santarem office for their extensive logistical and field assistance. Finally, we also thank the two anonymous reviewers whose useful comments improved the clarity of this paper. This work was supported by grants NASA NCC5-341 and NASA NCC5-684 to Harvard University.

References

Araújo, A. C., et al. (2002), Comparative measurements of carbon dioxide fluxes from two nearby towers in a central Amazonian rain forest: The Manaus LBA site, *J. Geophys. Res.*, *107*(D20), 8090, doi:10.1029/2001JD000676.

Baldocchi, D. D., B. B. Hicks, and T. P. Meyers (1988), Measuring biosphere-atmosphere exchanges of biologically related gases with micrometeorological methods, *Ecology*, *69*(5), 1331–1340.

Botta, A., N. Ramankutty, and J. A. Foley (2002), Long-term variations of climate and carbon fluxes over the Amazon basin, *Geophys. Res. Lett.*, *29*(9), 1319, doi:10.1029/2001GL013607.

Brown, S., and A. E. Lugo (1982), The storage and production of organic-material in tropical forests and their role in the global carbon-cycle, *Biotropica*, *14*(3), 161–187.

Carswell, F. E., et al. (2002), Seasonality in CO_2 and H_2O flux at an eastern Amazonian rain forest, *J. Geophys. Res.*, *107*(D20), 8076, doi:10.1029/2000JD000284.

Chambers, J. Q., N. Higuchi, J. P. Schimel, L. V. Ferreira, and J. M. Melack (2000), Decomposition and carbon cycling of dead trees in tropical forests of the central Amazon, *Oecologia*, *122*(3), 380–388.

Chambers, J. Q., et al. (2004), Respiration from a tropical forest ecosystem: Partitioning of sources and low carbon use efficiency, *Ecol. Appl.*, *14*(4), S72–S88.

Choudhury, B. J., and N. E. DiGirolamo (1998), A biophysical process-based estimate of global land surface evaporation using satellite and ancillary data-I. Model description and comparison with observations, *J. Hydrol.*, *205*, 164–185.

Clark, D. B. (1996), Abolishing virginity, *J. Trop. Ecol.*, *12*, 735–739.

da Rocha, H. R., M. L. Goulden, S. D. Miller, M. C. Menton, L. D. V. O. Pinto, H. C. de Freitas, and A. M. E. S. Figueira (2004), Seasonality of water and heat fluxes over a tropical forest in eastern Amazonia, *Ecol. Appl.*, *14*(4), S22–S32.

Davidson, E. A., and I. A. Janssens (2006), Temperature sensitivity of soil carbon decomposition and feedbacks to climate change, *Nature*, *440*, 165–173.

Davidson, E. A., F. Y. Ishida, and D. C. Nepstad (2004), Effects of an experimental drought on soil emissions of carbon dioxide, methane, nitrous oxide, and nitric oxide in a moist tropical forest, *Global Change Biol.*, *10*, 718–730.

Davidson, E. A., I. A. Janssens, and Y. Q. Luo (2006), On the variability of respiration in terrestrial ecosystems: moving beyond Q(10), *Global Change Biol.*, *12*(2), 154–164.

Dickinson, R. E., and A. Henderson-Sellers (1988), Modeling tropical deforestation—a study of GCM land surface parameterizations, *Q. J. R. Meteorol. Soc.*, *114*(480), 439–462.

Doughty, C. E., M. L. Goulden, S. D. Miller, and H. R. da Rocha (2006), Circadian rhythms constrain leaf and canopy gas exchange in an Amazonian forest, *Geophys. Res. Lett.*, *33*, L15404, doi:10.1029/2006GL026750.

FAO (1992), Third interim report on the state of tropical forests, Food and Agric. Org., Rome.

Finnigan, J. (2004), Advection and modeling, in *Handbook for Micrometeorology*, edited by X. Lee, W. Massman, and B. Law, Kluwer Acad., Dordrecht.

Freeland, R. O. (1952), Effect of age of leaves upon the rate of photosynthesis in some conifers, *Plant Physiol.*, *27*, 685–690.

Fung, I. Y., S. C. Doney, K. Lindsay, and J. John (2005), Evolution of carbon sinks in a changing climate, *Proc. Natl. Acad. Sci. U. S. A.*, *102*(32), 11,201–11,206.

Garstang, M., H. L. Massie, J. Halverson, S. Greco, and J. Scala (1994), Amazon coastal squall lines. 1. Structure and kinematics, *Mon. Weather Rev.*, *122*(4), 608–622.

Goulden, M. L., J. W. Munger, S. M. Fan, B. C. Daube, and S. C. Wofsy (1996), Measurements of carbon sequestration by long-term eddy covariance: methods and a critical evaluation of accuracy, *Global Change Biol.*, *2*, 169–182.

Goulden, M. L., S. D. Miller, H. R. da Rocha, M. C. Menton, H. C. Freitas, A. M. Figueira, and A. C. D. de Sousa (2004), Diel and seasonal patterns of tropical forest CO_2 exchange, *Ecol. Appl.*, *14*(4), S43–S54.

Gu, L. H., D. D. Baldocchi, S. C. Wofsy, J. W. Munger, J. J. Michalsky, S. P. Urbanski, and T. A. Boden (2003), Response of a deciduous forest to the Mount Pinatubo eruption: Enhanced photosynthesis, *Science*, *299*, 2035–2038.

Holdridge, L. R. (1947), Determination of world plant formations from simple climatic data, *Science*, *105*, 367–368.

Huete, A. R., et al. (2006), Amazon rain forests green-up with sunlight in dry season, *Geophys. Res. Lett.*, *33*, L06405, doi:10.1029/2005GL025583.

Hutyra, L. R., J. W. Munger, C. A. Nobre, S. R. Saleska, S. A. Vieira, and S. C. Wofsy (2005), Climatic variability and vegetation vulnerability in Amazonia, *Geophys. Res. Lett.*, *32*, L24712, doi:10.1029/2005GL024981.

Kaimal, J. C., Y. Izumi, J. C. Wyngaard, and R. Cote (1972), Spectral characteristics of surface-layer turbulence, *Q. J. R. Meteorol. Soc.*, *98*(417), 563–589.

Kruijt, B., et al. (2004), The robustness of eddy correlation fluxes for Amazon rain forest conditions, *Ecol. Appl.*, *14*(4), S101–S113.

Lee, J. E., R. S. Oliveira, T. E. Dawson, and I. Fung (2005), Root functioning modifies seasonal climate, *Proc. Natl. Acad. Sci. U. S. A.*, *102*(49), 17,576–17,581.

Lee, X., J. Finnigan, and K. T. Paw U (2004), Coordinate systems and flux bias error, in *Handbook of Micrometeorology: A Guide for Surface Flux Measurement and Analysis*, edited by W. M. X. Lee and B. Law, pp. 33–66, Kluwer Acad., Dordrecht.

Lu, L. X., A. S. Denning, M. A. da Silva-Dias, P. da Silva-Dias, M. Longo, S. R. Freitas, and S. Saatchi (2005), Mesoscale circulations and atmospheric CO_2 variations in the Tapajós Region, Para, Brazil, *J. Geophys. Res.*, *110*, D21102, doi:10.1029/2004JD005757.

Malhi, Y., A. D. Nobre, J. Grace, B. Kruijt, M. Pereira, A. Culf, and S. Scott (1998), Carbon dioxide transfer over a central Amazonian rain forest, *J. Geophys. Res.*, *103*, 31,593–31,612.

Malhi, Y., E. Pegoraro, A. D. Nobre, M. G. P. Pereira, J. Grace, A. D. Culf, and R. Clement (2002), Energy and water dynamics of a central Amazonian rain forest, *J. Geophys. Res.*, *107*(D20), 8061, doi:10.1029/2001JD000623.

Martens, C. S., et al. (2004), Radon fluxes in tropical forest ecosystems of Brazilian Amazonia; night-time CO_2 net ecosystem exchange derived from radon and eddy covariance methods., *Global Change Biol.*, *10*, 618–629.

McMillen, R. T. (1988), An eddy-correlation technique with extended applicability to non-simple terrain, *Boundary Layer Meteorol.*, *43*(3), 231–245.

Melillo, J. M., A. D. McGuire, D. W. Kicklighter, B. Moore, C. J. Vorosmarty, and A. L. Schloss (1993), Global climate-change and terrestrial net primary production, *Nature*, *363*, 234–240.

Mitchell, T. D., T. R. Carter, P. D. Jones, M. Hulme, and M. New (2003), A comprehensive set of grids of monthly climate data for Europe and the globe: the observed record (1901–2000) and 16 scenarios, working paper, 30 pp., Tyndall Cent., Norwich, UK.

Moore, C. J., and G. Fisch (1986), Estimating heat storage in Amazonian tropical forest, *Agric. For. Meteorol.*, *38*, 147–169.

Nascimento, H. E. M., and W. F. Laurance (2004), Biomass dynamics in Amazonian forest fragments, *Ecol. Appl.*, *14*(4), S127–S138.

Nepstad, D., et al. (2004), Amazon drought and its implication for forest flammability and tree growth; a basin-wide analysis, *Global Change Biol.*, *10*, 704–717.

Nepstad, D. C., et al. (1994), The role of deep roots in the hydrological and carbon cycles of Amazonian forests and pastures, *Nature*, *372*, 666–669.

Nepstad, D. C., et al. (2002), The effects of partial throughfall exclusion on canopy processes, aboveground production, and biogeochemistry of an Amazon forest, *J. Geophys. Res.*, *107*(D20), 8085, doi:10.1029/2001JD000360.

Oliveira, R. S., T. E. Dawson, S. S. O. Burgess, and D. C. Nepstad (2005), Hydraulic redistribution in three Amazonian trees, *Oecologia*, *145*(3), 354–363.

Parrotta, J. A., J. K. Francis, and De R. R. Almeida (1995), Trees of the Tapajós, U.S. Dep. of Agric., Rio Piedras, Puerto Rico.

Raich, J. W., and W. H. Schlesinger (1992), The global carbon-dioxide flux in soil respiration and its relationship to vegetation and climate, *Tellus, Ser. B*, *44*(2), 81–99.

Rice, A. H., et al. (2004), Carbon balance and vegetation dynamics in an old-growth Amazonian forest, *Ecol. Appl.*, *14*(4), s55–s71.

Richardson, A. D., and D. Y. Hollinger (2005), Statistical modeling of ecosystem respiration using eddy covariance data: Maximum likelihood parameter estimation, and Monte Carlo simulation of model and parameter uncertainty, applied to three simple models, *Agric. For. Meteorol.*, *131*(3–4), 191–208.

Rivera, G., S. Elliott, L. S. Caldas, G. Nicolossi, V. T. R. Coradin, and R. Borchert (2002), Increasing day-length induces spring flushing of tropical dry forest trees in the absence of rain, *Trees Struct. Funct.*, *16*(7), 445–456.

Saleska, S. R., et al. (2003), Carbon in Amazon forests: Unexpected seasonal fluxes and disturbance-induced losses, *Science*, *302*, 1554–1557.
Schaphoff, S., W. Lucht, D. Gerten, S. Sitch, W. Cramer, and I. C. Prentice (2006), Terrestrial biosphere carbon storage under alternative climate projections, *Clim. Change*, *74*(1–3), 97–122.
Shuttleworth, W. J. (1988), Evaporation from Amazonian rain forest, *Proc. R. Soc. London, Ser. B.*, *233*, 321–346.
Silver, W. L., J. Neff, M. McGroddy, E. Veldkamp, M. Keller, and R. Cosme (2000), Effects of soil texture on belowground carbon and nutrient storage in a lowland Amazonian forest ecosystem, *Ecosystems*, *3*, 193–209.
Tian, H. Q., J. M. Melillo, D. W. Kicklighter, A. D. McGuire, J. V. K. Helfrich, B. Moore, and C. J. Vorosmarty (1998), Effect of interannual climate variability on carbon storage in Amazonian ecosystems, *Nature*, *396*(6712), 664–667.
Trumbore, S. E. (2006), Carbon respired by terrestrial ecosystems - recent progress and challenges, *Global Change Biol.*, *12*(2), 141–153.
Vieira, S., et al. (2004), Forest structure and carbon dynamics in Amazonian tropical rain forests, *Oecologia*, *140*, 468–479.
von Randow, C., et al. (2004), Comparative measurements and seasonal variations in energy and carbon exchange over forest and pasture in South West Amazonia, *Theor. Appl. Climatol.*, *78*, 5–26.
Vourlitis, G. L., N. Priante, M. M. S. Hayashi, J. D. Nogueira, F. T. Caseiro, and J. H. Campelo (2002), Seasonal variations in the evapotranspiration of a transitional tropical forest of Mato Grosso, Brazil, *Water Resour. Res.*, *38*(6), 1094, doi:10.1029/2000WR000122.
Webb, E. K., G. I. Pearman, and R. Leuning (1980), Correction of flux measurements for density effects due to heat and water-vapour transfer, *Q. J. R. Meteorol. Soc.*, *106*, 85–100.
Werth, D., and R. Avissar (2004), The regional evapotranspiration of the Amazon, *J. Hydrometeorol.*, *5*, 100–109.
Wilson, K., et al. (2002), Energy balance closure at FLUXNET sites, *Agric. For. Meteorol.*, *113*(1–4), 223–243.
Wright, S. J., and C. P. van Schaik (1994), Light and the phenology of tropical trees, *Am. Nat.*, *143*, 192–199.

D. F. Amaral, LBA-ECO, Santarém, 68040050 Pará, Brazil.
B. C. Daube, A. L. Dunn, E. Gottlieb, J. W. Munger, and S. C. Wofsy, Department of Earth and Planetary Sciences, Harvard University, Cambridge, MA 02138, USA.
P. B. de Camargo, Laboratório de Ecologia Isotópica, CENA/USP, P.O. Box 96, Piracicaba, 13400-970 SP, Brazil.
L. R. Hutyra, Department of Urban Design and Planning, University of Washington, Seattle, WA 98195, USA. (lrhutyra@u.washington.edu)
S. R. Saleska, Department of Ecology and Evolutionary Biology, University of Arizona, Tucson, AZ 85721, USA.